Graphene Oxide as a Sulfur Immobilizer in High Performance Lithium/Sulfur Cells

Liwen Ji,[†,□] Mumin Rao,[‡,□,¶] Haimei Zheng,[§] Liang Zhang,[⊥,○] Yuanchang Li,[∥] Wenhui Duan,[∥] Jinghua Guo,[⊥] Elton J. Cairns,[‡] and Yuegang Zhang[*,†]

[†]The Molecular Foundry, Lawrence Berkeley National Laboratory, Berkeley, California 94720, United States

[‡]Environmental Energy Technologies Division, Lawrence Berkeley National Laboratory, Berkeley, California 94720, United States and Department of Chemical and Biomolecular Engineering, University of California, Berkeley, California 94720, United States

[§]Materials Sciences Division, Lawrence Berkeley National Laboratory, Berkeley, California 94720, United States

[⊥]The Advanced Light Source, Lawrence Berkeley National Laboratory, Berkeley, California 94720, United States

[∥]Department of Physics, Tsinghua University, Beijing 100084, China

S *Supporting Information*

ABSTRACT: The loss of sulfur cathode material as a result of polysulfide dissolution causes significant capacity fading in rechargeable lithium/sulfur cells. Here, we use a chemical approach to immobilize sulfur and lithium polysulfides via the reactive functional groups on graphene oxide. This approach enabled us to obtain a uniform and thin (around tens of nanometers) sulfur coating on graphene oxide sheets by a simple chemical reaction—deposition strategy and a subsequent low-temperature thermal treatment process. Strong interaction between graphene oxide and sulfur or polysulfides enabled us to demonstrate lithium/sulfur cells with a high reversible capacity of $950-1400$ mA h g^{-1}, and stable cycling for more than 50 deep cycles at 0.1C (1C = 1675 mA g^{-1}).
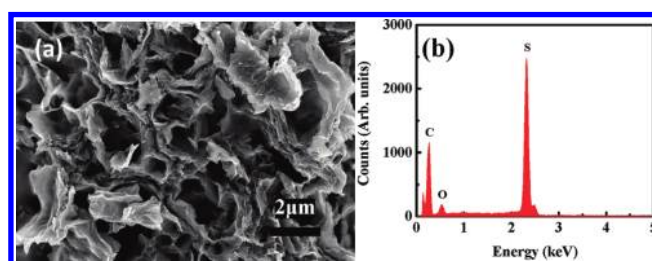
Figure 1. SEM image (a) and EDX spectrum (b) of the GO-S nanocomposite after heat treatment in Ar at 155 °C for 12 h.

demonstrated that the mesoporous carbon/S nanocomposites can be cycled for 100 cycles at 974 mA h g^{-1} at a rate of 0.5C (1C = 1675 mA g^{-1}) with the corresponding coulombic efficiency of ~96% and 94%, respectively, at the first and 100th cycles.[23] Despite this progress, there are still few reports on fabricating novel C—S cathodes via the chemical reaction approach.[14]

In this work, we used a low-cost and environmentally benign chemical reaction—deposition strategy to immobilize S on quasi-two-dimensional graphene oxides (GO) to prepare graphene oxide—sulfur (GO-S) nanocomposite cathodes for Li/S cells in ionic liquid-based electrolytes. We first deposited nano-S onto graphene oxide (GO) sheets by chemical reaction in a micro-emulsion system (see experimental section in the Supporting Information [SI] for details). Then, we heat treated the as-synthesized samples in an argon (Ar) environment at low temperature (155 °C) for 12 h in order to remove some of the bulk S which is not directly attached to the GO layers. When the as-synthesized GO-S nanocomposites were heat-treated in Ar, the bulk S on the external surface of the GO melted and diffused into the pores of the GO due to the strong adsorption effects derived from both the high surface area and the functional groups on the surface of the GO. At the same time, this low-temperature heat treatment process can partially remove and/or chemically modify some of the functional groups on the GO surface and

E lemental sulfur (S) is very attractive as a cathode material for high-specific-energy rechargeable lithium batteries, because a battery based on the lithium/sulfur (Li/S) couple would yield a theoretical specific capacity of about 1675 mA h g^{-1} with a theoretical specific energy of 2600 W h kg^{-1} on the assumption of the complete reaction of Li with S to form Li$_2$S. In addition, S is also inexpensive, abundant, and nontoxic. Therefore, S is a promising cathode material for high specific energy Li/S batteries.[1−15] Despite these considerable advantages, there are still a number of challenges in Li/S batteries. The first one is the high electrical resistivity of elemental S. The second one is the high solubility (in organic solvent electrolytes) of the polysulfide ions that are formed during the discharge/charge processes. The soluble intermediate Li polysulfides can diffuse through the electrolyte to the Li anode where they are reduced to form solid precipitates (such as Li$_2$S or Li$_2$S$_2$). These reduced products can also diffuse back to the cathode during recharging. These issues can lead to low active materials utilization, low coulombic efficiency, and short cycle life of the S electrode.[1−15] In order to address these challenges, various carbon and conductive polymer materials have been used to accommodate S, to overcome its insulating property and reduce the dissolution of Li polysulfides, as reported by Nazar, et al.[1,13,15] and others.[4,6,7,10,12,16−22] The most recent work by Archer et al.
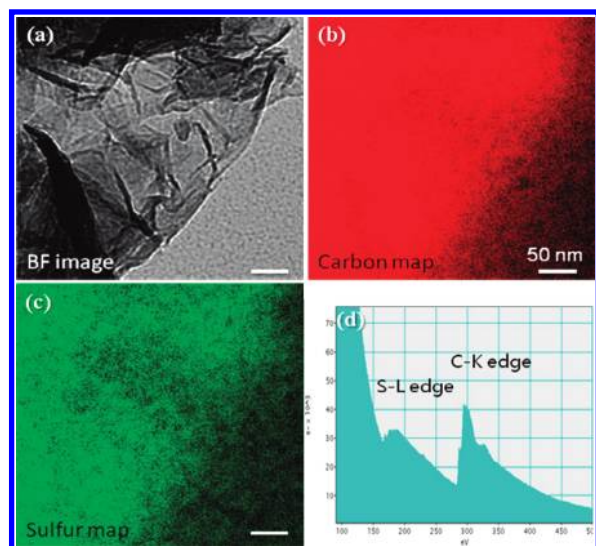
Figure 2. TEM bright field (BF) image (a) and the corresponding elemental mapping for carbon (b) and S (c) reveal a homogeneous S coating on the GO flakes. EELS spectrum is shown in (d). The scale bars are 50 nm.

improve the electronic conductivity of the as-prepared GO-S nanocomposites (see Table 1 in the SI).

Figure 1a shows the scanning electron microscope (SEM) image of the as-prepared GO-S nanocomposite after heat treatment. The layer-like extremely conjugated nanostructures with highly developed porous structures are clearly illustrated. The energy-dispersive X-ray (EDX) microanalysis in Figure 1b confirms the existence of S in the composite. As indicated in the thermogravimetric analysis (TGA), about 66 wt % S is incorporated into the GO after heat treatment (Figure S1, SI). The transmission electron microscope (TEM) image in Figure 2a and the electron energy-loss spectrum (EELS) in Figure 2d indicate that a thin layer of S with a thickness of tens of nanometers is homogenously dispersed on the flake-like GO surface with no significant fraction of bulk S exposed on the external surface of the sample after heat treatment (For comparison, see the SEM images for pure GO and SEM/TEM images for GO-S nanocomposites in Figures S2 and S3 (SI) before heat treatment). The corresponding elemental mapping of carbon (Figure 2b), and S (Figure 2c) display a very similar intensity distribution, revealing a homogeneous S coating on the GO flakes in the as-formed GO-S nanocomposites.

The unique structure of the GO-S nanocomposite can improve the overall electrochemical performance when it is used as a cathode material for Li/S batteries. First, it can accommodate the significant volume changes of S as it is converted to Li_2S on discharge, and back to elemental S on recharge.[1−10,17,24] In addition, the partially reduced GO with its large surface area along with ubiquitous cavities can establish more intimate electronic contact with S and avoid aggregation and loss of electrical contact with the current collector. Second, the low-temperature heat-treated GO still contains various kinds of functional groups (Figure S5, SI).These functional groups can have strong adsorbing ability to anchor S atoms and to effectively prevent the subsequently formed Li polysulfides from dissolving in the electrolyte during cycling.

We performed ab initio calculations to clarify the role of functional groups on GO in immobilizing S (see the calculation methods and detailed results in the SI). The results indicated that
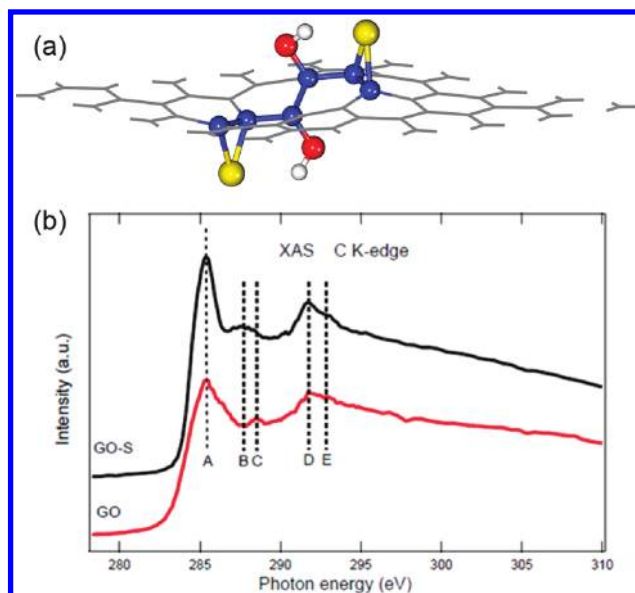

Figure 3. (a) Representative pattern of GO immobilizing S. The hydroxyl enhances the binding of S to the C−C bond due to the induced ripples by epoxy or hydroxyl group. Yellow, red, and white balls denote S, O, and H atoms, respectively, while the others are C atoms. Note that the C atoms bonding to S or O are highlighted as blue balls. (b) C K-edge XAS spectra of GO and GO-S nanocomposites after heat treatment in Ar at 155 °C for 12 h.
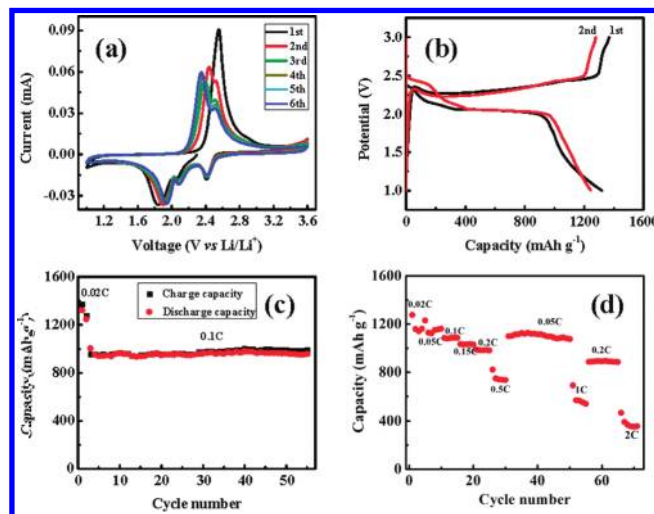

Figure 4. (a) CV curve at 0.05 mV s^{-1} scanning rate; (b) galvanostatic discharge/charge profiles at 0.02C rate; (c) cycling performance at a constant current rate of 0.1C after initial activation processes at 0.02C for two cycles; (d) reversible capacity vs current density (rate capability). The GO-S nanocomposites were heat treated in Ar environment at 155 °C for 12 h.

both epoxy and hydroxyl groups can enhance the binding of S to the C−C bonds due to the induced ripples by the functional groups (Figure 3a). We also performed soft X-ray absorption spectroscopy (XAS) measurement which probes unoccupied electronic structure and thus is a powerful tool for probing chemical bonding in surface chemistry. Figure 3b shows the carbon K-edge absorption spectra for both GO and GO-S nanocomposites (see S K-edge spectrum in Figure S7, SI). The absorption features "A", "D", and

"E", which can be attributed to the π^* state, excitonic state, and σ^* state,[25] are observed for both samples. Of note in the spectra is the increase in the sharpness of the π^* and excitonic state for GO-S nanocomposites as compared with GO, suggesting that the ordering of the sp^2-hybridized carbon structure is better formatted after S is incorporated. In addition, feature "C" originating from a different functional group (possibly the C—O bond) on the GO are weakened significantly when incorporated with S, which means strong chemical interaction between S and the functional group of GO happens and S can partially reduce the GO.[26] Besides, a new feature "B", originating from the C—S σ^* excitations,[27] is observed for the GO-S nanocomposites.

We evaluated the electrochemical Li storage capability of these heat-treated GO-S nanocomposites as potential cathode materials for Li/S cells in the n-methyl-(n-butyl) pyrrolidinium bis-(trifluoromethanesulfonyl)imide (PYR$_{14}$TFSI), Li-bis(trifluoro-methylsulfonyl)imide (LiTFSI), and poly(ethylene glycol) dimethyl ether (PEGDME, $M_w = 250$) mixture-based electrolyte. Figure 4a shows the cyclic voltammetry (CV) profile of one electrode. The measurement was conducted at a scan rate of 0.05 mV s^{-1} in the voltage range of 1.0 to 3.6 V vs Li/Li$^+$. During the first cathodic scan, three main reduction peaks at around 2.4, 2.1, and 1.8 V were clearly shown. According to the reported mechanisms for oxidation and reduction of S during discharge/charge,[5,6,10,18,19,28−31] the peak at around 2.4 V can be assigned to the reduction of elemental S to higher-order Li polysulfides (Li$_2$S$_n$, $n \geq 8$). The peak at about 2.1 V probably corresponds to the reduction of higher-order Li polysulfides to lower-order Li polysulfides (such as Li$_2$S$_6$, Li$_2$S$_4$) from Li$_2$S$_8$.[5,6,10,16−21,28−31] The peak at 1.8 V is related to the reduction of polysulfide species to form Li$_2$S. In the subsequent anodic scan, only one sharp oxidation peak is observed at about 2.6 V that is attributed to the complete conversion of Li$_2$S and polysulfides into elemental S. The main reduction peak is shifted to slightly higher potential and the oxidation peaks to lower potentials with increase in cycle number, indicating an improvement of reversibility of the cell with cycling. In addition, as the cycle number increased, the oxidation peak at 2.6 V becomes less significant, while another new one at 2.35 V grows higher in intensity. The oxidation peak at 2.35 V is associated with the formation of Li$_2$S$_n$ ($n > 2$).[23,29] After the second cycle, both the CV peak positions and peak currents undergo very small changes, indicating relatively good capacity retention. The CV results show that GO can help to prevent S from dissolving into the electrolyte because of its large surface along with some functional groups on the surface.

Figure 4b depicts the first and second cycle discharge/charge typical voltage profiles of the electrodes at the 0.02C rate (1C = 1675 mA g^{-1}) between 1.0 and 3.0 V. (The capacity values in this article are calculated according to the mass of S.) All the discharge curves show three plateaus in the voltage profile that are consistent with the peaks in the CV and are also well documented in the literature.[5,6,10,16,18−21,23,28] The GO-S nanocomposite delivers a high initial discharge capacity of about 1320 mA h g^{-1} at 0.02C. The corresponding coulombic efficiency in the first discharge/charge cycle is 96.4%. At the second cycle, a large reversible capacity of about 1247 mA h g^{-1} is preserved (97.5% coulombic efficiency), corresponding to about 94.5% capacity retention. This initial capacity loss is small compared to the formerly reported results of similar materials,[16,32] indicating that the strong GO-S interaction can reduce the dissolution of the lithium polysulfides into the electrolyte and thus minimize the shuttle phenomenon. Figure 4c shows the cycling performance of

the same cell cycled at a rate of 0.1C after the initial two cycles at 0.02C. The discharge capacity of the first cycle at 0.1C remains at around 1000 mA h g^{-1}. At the second cycle at 0.1C, this value decreases to about 950 mA h g^{-1}. However, after more than 50 cycles at the same rate, the reversible capacity remains at 954 mA h g^{-1}(with a coulombic efficiency of about 96.7%), indicating very stable reversibility of the electrochemical reactions and excellent capacity retention (also see the cycle performance of another coin cell in Figure S10, SI). The GO-S nanocomposites display improved coulombic efficiencies compared to the former reports.[23]

The discharge capacity of the GO-S was highly reproducible over many coin cells. Another example of the electrochemical performance of the GO-S electrode is demonstrated in Figure 4d where a cell showed a reversible capacity of 735 mA h g^{-1} at 0.5C after 30 cycles at various rates. Further cycling at a low rate of 0.05 C brings it back to a reversible capacity of about 1100 mA h g^{-1} for another 20 cycles. When this coin cell was discharged at a higher rate of 1C, a reversible capacity of about 550 mA h g^{-1} was obtained. The last decrease of the rate to 0.2C, yielded a reversible capacity of about 890 mA h g^{-1}. When this coin cell was further discharged at 2C, an acceptable reversible capacity of about 370 mA h g^{-1} was obtained, indicating excellent capacity reversibility and high rate performance (see the corresponding discharge/charge profiles in Figure S11, SI.)

The GO clearly performs very well as a means to stabilize the S electrode. The GO provides highly reactive functional groups on its surface that can serve as immobilizers to hold the S.[1,5,8] Also, by limiting the concentration of the polysulfide anions in the electrolyte, the redox shuttle phenomenon is largely avoided.[1,8,9] The intimate contact of the S provided by the large surface area and the functional groups on GO is favorable to good electron/ion accessibility, leading to enhanced cycle performance and rate capability.[1−9,17,20] In addition, the optimized ionic liquid-based electrolytes which have suitable viscosities and wetting properties influence the penetration of electrolyte into the S electrode structure, while increasing the ionic conductivity within the electrodes at the same time (see control experiment in LiTFSI-PEGDME-based electrolyte in Figure S12, SI).[5,33,34]

In summary, a novel chemical approach is employed to synthesize a GO-S nanocomposite to immobilize S in the cathode material of Li/S cells. The GO-S nanocomposite cathodes display good reversibility, excellent capacity stability of about 1000 mA h g^{-1}, and rate capability of up to 2C in ionic liquid-based electrolyte. The GO in the heat-treated composites has good conductivity and an extremely high surface area, and provides a robust electron transport network. The functional groups on the GO surface play the role of immobilizers that keep intimate contact of the conducting matrix with S species, and effectively confine any polysulfides from dissolving. The GO network also accommodates the volume change of the electrode during the Li—S electrochemical reaction. As a result, reversibility and high rate discharge capability were obtained. The same strategy could be helpful to explore and develop new porous carbon[35,36] or conductive polymer-based S nanocomposite cathodes for advanced Li/S cells.

■ ASSOCIATED CONTENT

Ⓢ Supporting Information. Experimental methods, TGA, XAS, SME, TEM, and calculation results. This material is available free of charge via the Internet at http://pubs.acs.org.

18524

dx.doi.org/10.1021/ja206955k |J. Am. Chem. Soc. 2011, 133, 18522–18525

■ AUTHOR INFORMATION

Corresponding Author
yzhang5@lbl.gov

Author Contributions
□These authors contributed equally to this work.

Notes
¶M.R. is a visiting researcher from South China University of Technology.
○L.Z. is a visiting researcher from University of Science and Technology of China.

■ REFERENCES

(1) Ji, X.; Lee, K. T.; Nazar, L. F. *Nat. Mater.* **2009**, *8*, 500–506.
(2) Hassoun, J.; Scrosati, B. *Angew. Chem., Int. Ed.* **2010**, *122*, 2421–2424.
(3) Kolosnitsyn, V.; Karaseva, E. *Russ. J. Electrochem.* **2008**, *44*, 506–509.
(4) Yang, Y.; McDowell, M. T.; Jackson, A.; Cha, J. J.; Hong, S. S.; Cui, Y. *Nano Lett.* **2010**, *10*, 1486–1491.
(5) Shim, J.; Striebel, K. A.; Cairns, E. J. *J. Electrochem. Soc.* **2002**, *149*, A1321–A1325.
(6) Choi, Y.-J.; Chung, Y.-D.; Baek, C.-Y.; Kim, K.-W.; Ahn, H.-J.; Ahn, J.-H. *J. Power Sources* **2008**, *184*, 548–552.
(7) Liang, C.; Dudney, N. J.; Howe, J. Y. *Chem. Mater.* **2009**, *21*, 4724–4730.
(8) Ji, X.; Nazar, L. F. *J. Mater. Chem.* **2010**, *20*, 9821–9826.
(9) Gao, X.-P.; Yang, H.-X. *Energy Environ. Sci.* **2010**, *3*, 174–189.
(10) Lai, C.; Gao, X. P.; Zhang, B.; Yan, T. Y.; Zhou, Z. *J. Phys. Chem. C* **2009**, *113*, 4712–4716.
(11) Ryu, H.-S.; Ahn, H.-J.; Kim, K.-W.; Ahn, J.-H.; Lee, J.-Y. *J. Power Sources* **2006**, *153*, 360–364.
(12) Wang, J.; Yang, J.; Xie, J.; Xu, N. *Adv. Mater.* **2002**, *14*, 963–965.
(13) Ji, X.; Evers, S.; Black, R.; Nazar, L. F. *Nat. Commun.* **2011**, *2*, 325.
(14) Wang, H.; Yang, Y.; Liang, Y.; Robinson, J. T.; Li, Y.; Jackson, A.; Cui, Y.; Dai, H. *Nano Lett.* **2011**, *11*, 2644–2647.
(15) He, G.; Ji, X.; Nazar, L. *Energy Environ. Sci.* **2011**, *4*, 2878–2883.
(16) Cao, Y.; Li, X.; Aksay, I. A.; Lemmon, J.; Nie, Z.; Yang, Z.; Liu, J. *Phys. Chem. Chem. Phys.* **2011**, *13*, 7660–7665.
(17) Chen, S.-R.; Zhai, Y.-P.; Xu, G.-L.; Jiang, Y.-X.; Zhao, D.-Y.; Li, J.-T.; Huang, L.; Sun, S.-G. *Electrochim. Acta* **2011**, *56*, 9549–9555.
(18) Jeon, B. H.; Yeon, J. H.; Kim, K. M.; Chung, I. J. *J. Power Sources* **2002**, *109*, 89–97.
(19) Liang, X.; Wen, Z.; Liu, Y.; Zhang, H.; Huang, L.; Jin, J. *J. Power Sources* **2011**, *196*, 3655–3658.
(20) Wang, J.; Chew, S. Y.; Zhao, Z. W.; Ashraf, S.; Wexler, D.; Chen, J.; Ng, S. H.; Chou, S. L.; Liu, H. K. *Carbon* **2008**, *46*, 229–235.
(21) Yuan, L. X.; Feng, J. K.; Ai, X. P.; Cao, Y. L.; Chen, S. L.; Yang, H. X. *Electrochem. Commun.* **2006**, *8*, 610–614.
(22) Wang, J.; Chen, J.; Konstantinov, K.; Zhao, L.; Ng, S. H.; Wang, G. X.; Guo, Z. P.; Liu, H. K. *Electrochim. Acta* **2006**, *51*, 4634–4638.
(23) Jayaprakash, N.; Shen, J.; Moganty, S. S.; Corona, A.; Archer, L. A. *Angew. Chem., Int. Ed.* **2011**, *50*, 5904–5908.
(24) Ji, L.; Tan, Z.; Kuykendall, T. R.; Aloni, S.; Xun, S.; Lin, E.; Battaglia, V.; Zhang, Y. *Phys. Chem. Chem. Phys.* **2011**, *13*, 7170–7177.
(25) Skytt, P.; Glans, P.; Mancini, D. C.; Guo, J. H.; Wassdahl, N.; Nordgren, J.; Ma, Y. *Phys. Rev. B* **1994**, *50*, 10457.
(26) Chen, W.; Yan, L.; Bangal, P. R. *J. Phys. Chem. C* **2010**, *114*, 19885–19890.
(27) Pasquali, L.; Terzi, F.; Montecchi, M.; Doyle, B. P.; Lukkari, J.; Zanfrognini, B.; Seeber, R.; Nannarone, S. *J. Electron Spectrosc. Relat. Phenom.* **2009**, *172*, 114–119.
(28) Yamin, H.; Peled, E. *J. Power Sources* **1983**, *9*, 281–287.
(29) Aurbach, D.; Pollak, E.; Elazari, R.; Salitra, G.; Kelley, C. S.; Affinito, J. *J. Electrochem. Soc.* **2009**, *156*, A694–A702.
(30) Jung, Y.; Kim, S. *Electrochem. Commun.* **2007**, *9*, 249–254.
(31) He, X.; Pu, W.; Ren, J.; Wang, L.; Wang, J.; Jiang, C.; Wan, C. *Electrochim. Acta* **2007**, *52*, 7372–7376.
(32) Wang, J.-Z.; Lu, L.; Choucair, M.; Stride, J. A.; Xu, X.; Liu, H.-K. *J. Power Sources* **2011**, *196*, 7030–7034.
(33) Shin, J. H.; Cairns, E. J. *J. Power Sources* **2008**, *177*, 537–545.
(34) Shin, J. H.; Cairns, E. J. *J. Electrochem. Soc.* **2008**, *155*, A368–A373.
(35) Long, J. W.; Dunn, B.; Rolison, D. R.; White, H. S. *Chem. Rev.* **2004**, *104*, 4463–4492.
(36) Ji, L.; Lin, Z.; Alcoutlabi, M.; Zhang, X. *Energy Environ. Sci.* **2011**, *4*, 2682–2699.

18525

dx.doi.org/10.1021/ja206955k |*J. Am. Chem. Soc.* 2011, 133, 18522–18525